Analyst

Accepted Manuscript

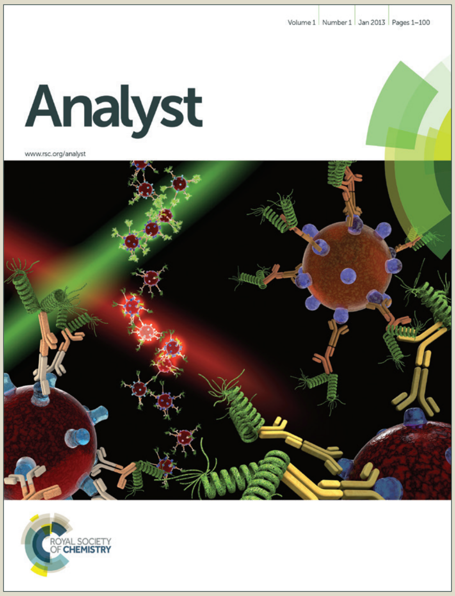

Journal Name

Dynamic Article Links ►

Cite this: DOI: 10.1039/c0xx00000x

www.rsc.org/xxxxxx

ARTICLE TYPE

Highly efficient quenching of tris(2,2'-bipyridyl)ruthenium(II) electrochemiluminescence using formaldehyde, methylglyoxal, and glyoxalate as coreactants by ozone and its application for ozone sensing

Ying Gao,[a] Xiaoyun Liu,[a,b] Wenjing Qi,[b,c] Wenyue Gao,[b,c] Yunhui Li*[a] and Guobao Xu*[b]

Received (in XXX, XXX) Xth XXXXXXXXX 20XX, Accepted Xth XXXXXXXXX 20XX

DOI: 10.1039/b000000x

Most electrochemiluminescence (ECL) systems require high concentrations of quencher to totally quench ECL. In this study, we found that ozone can quench the tris(2,2'-bipyridiyl)ruthenium(II) ECL using formaldehyde, methylglyoxal, or glyoxalate as coreactants at glassy carbon electrode with remarkable efficiencies even the concentration of ozone is merely 0.25% of that of these coreactants. The strongest quenching is observed with the tris(2,2'-bipyridiyl)ruthenium(II)/formaldehyde ECL system. The tris(2,2'-bipyridiyl)ruthenium(II)/formaldehyde ECL intensities decrease linearly with the ozone concentrations over the range of 0.025-25 μM (*r* = 0.9947) with a limit of detection of 8 nM. The method is more sensitive and faster than most methods. It shows high selectivity against other ROS or oxidants and some metal ions, such as H_2O_2, ClO^-, Mg^{2+}, Ni^{2+}, etc. The method exhibits high recoveries for the detection of ozone in a ventilated photocopy room.

Introduction

Recently, among various reactive oxygen species (ROS), ozone has been placed in the spotlight [1-4]. Ozone can dissolve in water and is an oxidant whose strength is nearly equal to fluorine. Therefore, ozone has been used in many fields involving medical tools, water treatment and food processing. However, ozone is harmful to human health [5, 6]. Therefore various detection methods of ozone have been reported [7-11]. Indigo carmine (IDS) colorimetric method is usually interfered by other oxidants. Titration-based techniques have low sensitivity. Several electrochemical methods have also been reported, and all electrochemical methods for ozone detection need modified electrodes [12, 13].

Electrochemiluminescence (ECL), also called electrogenerated chemiluminescence, is the light-emitting process resulting from the reaction of electrogenerated species [14-16]. ECL has excellent advantages, such as high sensitivity and wide dynamic range [17-20]. $Ru(bpy)_3^{2+}$ is one of most popular ECL reagents in aqueous solutions. Generally, $Ru(bpy)_3^{2+}$ ECL has two main categories, annihilation ECL [21] and coreactant ECL [22, 23]. Coreactant ECL occurs in a single-potential step by using coreactants, and is superiorly important for analytical applications [24, 25]. It has been extensively used for immunoassay [26], aptasensor [27], DNA detection [28], enzymatic biosensors [29], and the detection of many coreactants [30, 31]. Coreactant ECL can also be quenched by some compounds [32, 33], which has been utilized for analysis. For example, indigo carmine can quench the ECL of $Ru(phen)_3^{2+}$-doped silica nanoparticles and ozone can cleave indigo carmine to enhance ECL, enabling the detection of ozone [32]. However, the concentrations of quenchers are generally higher than the concentrations of coreactant in order to totally quench ECL, and thus limit the sensitivity for the detection of quenchers. Recently, we have found that ozone can nearly quench ECL of tris(1,10-phenanthroline)ruthenium(II)/glyoxal totally at ozone/glyoxal ratios less than 0.5 % because of the spontaneous polymerization of glyoxal in alkaline solution, and such remarkable quenching allows sensitive and facile ozone ECL detection without the time-consuming and complex synthesis of $Ru(phen)_3^{2+}$-doped silica nanoparticles [23]. It is desired to investigate the quenching effects of ozone on ECL using other polymerizable coreactants and to develop new efficient quenching systems.

In this study, the quenching effects of ozone on $Ru(bpy)_3^{2+}$ ECL using coreactants including formaldehyde, methylglyoxal, and glyoxalate were investigated. Ozone can dramatically inhibit $Ru(bpy)_3^{2+}$ ECL of these coreactants even the ozone concentration is much lower than the concentration of these coreactants, and shows strongest quenching efficiency on ECL of $Ru(bpy)_3^{2+}$/formaldehyde. The remarkable quenching efficiencies probably result from the unique property of these coreactants that can form oligomers in aqueous solutions. The applications of quenching effect on $Ru(bpy)_3^{2+}$/formaldehyde ECL for the detection of ozone were studied. The proposed method exhibits high sensitivity and selectivity and speediness.

Experimental section

Chemicals and Reagent

Tris(2,2'-bipyridyl)ruthenium(II) chloride was obtained from Sigma. Formaldehyde was purchased from Yili Chemical Reagent Factory (Beijing, China). Ozone was generated with an FMC900 ozone generator (BEYOK ozone, Zhejiang, China). Ozone solutions were prepared in a beaker filled with ice water to keep the stability of ozone in solutions. Using UV absorption detect the concentrations of ozone (λ_{max} = 258 nm; ε ≈ 3000 L mol^{-1} ·cm^{-1}). Supporting electrolyte is phosphate buffer solution (PBS) (0.2 M). Other chemicals were analytical-reagent grade and used as received. Doubly distilled water was used throughout the experiments.

Apparatus

Electrochemical experiments were carried out using a model CHI 660C electrochemical working station (Shanghai CHI Instruments Co., China). ECL intensities were performed using a BPCL ultra-weak luminescence analyzer. All experiments were carried out with a homemade three-electrode electrochemical cell system. The glassy carbon electrode (GCE), platinum wire, and Ag/AgCl (saturated with KCl) were used as working, counter, and reference electrodes, respectively. Unless otherwise noted, the photomultiplier tube voltage is biased at 1000 V.

Procedure of ozone detection

20 μL of 500 mM formaldehyde, 100 μL of 10 mM Ru(bpy)$_3^{2+}$, 200 μL of 0.2 M PBS (pH 10.0), different concentrations of ozone solutions and an appropriate amount of doubly distilled water were injected into a 1.0 mL plastic tube to ensure the whole volume of 1.0 mL. Then the solution was vortex-mixed and applied for ECL detection after 1 min.

Detection of ozone in indoor air samples

0.3 mL of 500 mM formaldehyde, 3 mL of 0.2 M PBS (pH 10.0) were injected into a 50 mL plastic tube. Then put the plastic tube in a ventilated photocopy room with five multifunctional printers. After nine hours, removed the sample and divided it into several parts, then added 100 μL of 10 mM Ru(bpy)$_3^{2+}$ and diluted with doubly distilled water to keep the final concentration of formaldehyde at 10 mM. One part was applied for ECL measurement of ozone. The other parts were applied for the detection of recoveries by adding given amounts of ozone into the sample solutions.

Results and discussion

Effect of ozone on tris(2,2'-bipyridiyl)ruthenium(II) ECL using formaldehyde, methylglyoxal, or glyoxalate as coreactants

Fig. 1a shows the ECL intensity of 1 mM Ru(bpy)$_3^{2+}$ is very weak. The addition of 25 μM ozone to 1 mM Ru(bpy)$_3^{2+}$ has little effect on ECL intensity (Fig 1b). In contrast, the addition of formaldehyde to 1 mM Ru(bpy)$_3^{2+}$ increases ECL intensity by about 100 times (Fig 1c). It indicates that ozone cannot serve as an efficient ECL coreactant and formaldehyde is an efficient coreactant. The ECL intensity of Ru(bpy)$_3^{2+}$/formaldehyde decreases to only about 5% although the ozone concentration is merely 0.25% of formaldehyde concentration (Fig 1d). Ozone can also efficiently inhibit ECL of Ru(bpy)$_3^{2+}$/methylglyoxal and Ru(bpy)$_3^{2+}$/glyoxalate. The ECL intensities of Ru(bpy)$_3^{2+}$/methylglyoxal and Ru(bpy)$_3^{2+}$/glyoxalate decrease to only about 11.6% and 11.7% , respectively. Since ozone exhibits strongest quenching effect on Ru(bpy)$_3^{2+}$/ formaldehyde ECL, Ru(bpy)$_3^{2+}$/ formaldehyde ECL was used for subsequent study.

To investigate the quenching mechanism, the corresponding cyclic voltammograms (CVs) were measured (Fig. 2). Ru(bpy)$_3^{2+}$ shows a pair of redox waves. The addition of 25 μM ozone to 1 mM Ru(bpy)$_3^{2+}$ does not affect the electrochemistry of Ru(bpy)$_3^{2+}$. The addition of formaldehyde to 1 mM Ru(bpy)$_3^{2+}$ result in the increase in oxidation peak and decrease in reduction peak (Fig 2c), indicating that Ru(bpy)$_3^{2+}$ can catalyze the oxidation of formaldehyde in alkaline solutions. The comparison of Fig 2c and Fig 2d demonstrates that ozone can inhibit the electrochemical oxidation formaldehyde (Fig 2d). It has well-documented that formaldehyde can spontaneously form polyformaldehyde in alkaline solutions. Since ozone concentration is much lower than formaldehyde, it suggests that ozone may react with polyformaldehyde and thus dramatically quench ECL through polymer amplification effect (Scheme 1)[23].

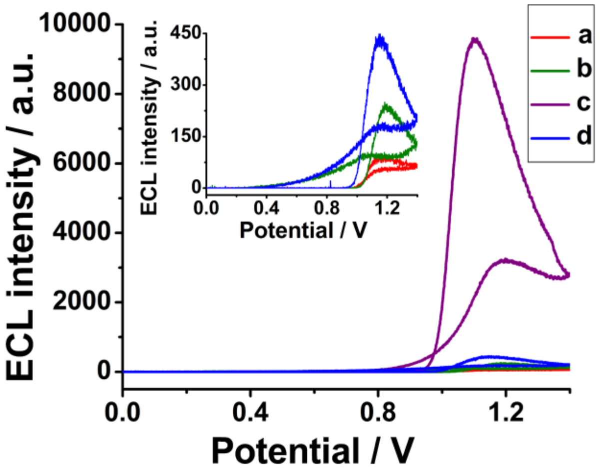

Fig. 1 ECL intensities at glassy carbon electrode (a) 1 mM Ru(bpy)$_3^{2+}$ (b) 1 mM Ru(bpy)$_3^{2+}$ + 25 μM ozone (c) 1 mM Ru(bpy)$_3^{2+}$ + 10 mM formaldehyde (d) 1 mM Ru(bpy)$_3^{2+}$ + 10 mM formaldehyde + 25 μM ozone. Conditions: PBS: 0.2 M, pH 10.0; Scan rate: 0.1 V/s, Photomultiplier tube voltage: 1000 V.

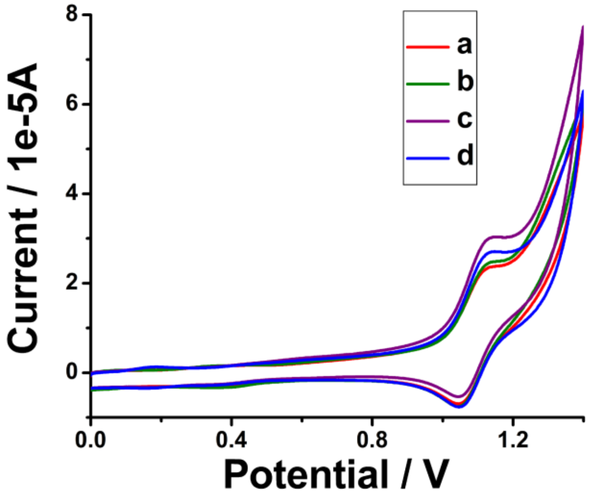

Fig. 2 Cyclic voltammograms at glassy carbon electrode (a) 1 mM Ru(bpy)$_3^{2+}$ (b) 1 mM Ru(bpy)$_3^{2+}$ + 25 μM ozone (c) 1 mM Ru(bpy)$_3^{2+}$ + 10 mM formaldehyde (d) 1 mM Ru(bpy)$_3^{2+}$ + 10 mM formaldehyde + 25 μM ozone. Conditions: PBS: 0.2 M, pH 10.0; Scan rate: 0.1 V/s, Photomultiplier tube voltage: 1000 V.

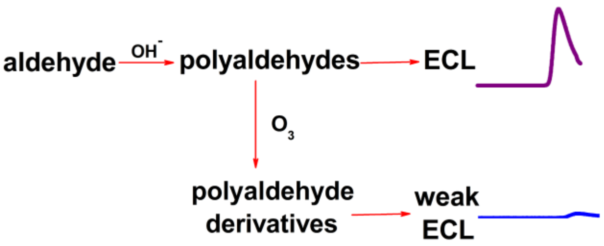

Scheme 1 Mechanism of ECL quenching by ozone.

pH effect on ECL behavior

Fig. 3 shows the effect of pH on the ECL inhibition efficiencies by ozone. *I* represents the ECL intensity of $Ru(bpy)_3^{2+}$/formaldehyde system after adding ozone; I_0 represents the ECL intensity of the control sample; $(I_0 - I)/I_0$ represents the ECL inhibition efficiency after adding ozone. The $(I_0 - I)/I_0$ increased significantly with pH value from 7.5 to 10.0 as shown in Fig. 3, and then tending towards stability when the pH value of buffer was larger than 10.0. Therefore, a pH of 10.0 was used in the following ozone detection experiments. The increase in the ECL inhibition efficiencies by ozone with increasing pH is ascribed to easier formation of polyformaldehyde at higher pH.

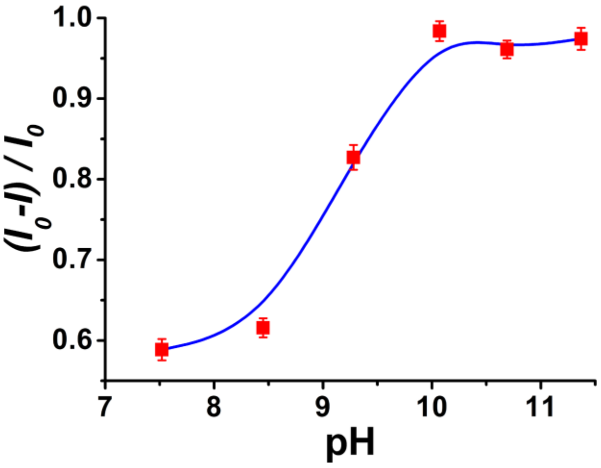

Fig. 3 Effect of pH on the ECL inhibition efficiencies by ozone at glassy carbon electrode. Conditions: *c*($Ru(bpy)_3^{2+}$): 1.0 mM; *c*(formaldehyde): 10 mM; *c*(ozone): 25 μM; PBS: 0.2 M; Scan rate: 0.1 V/s, Photomultiplier tube voltage: 1000 V.

Kinetic behavior of the ozone detection system

Fig. 4 shows the kinetic behavior of $Ru(bpy)_3^{2+}$/formaldehyde system for detecting ozone, which was investigated from 1 min to 30 min. The ECL intensity of $Ru(bpy)_3^{2+}$/formaldehyde system is very stable after formaldehyde and $Ru(bpy)_3^{2+}$ being mixed over 30 min, reflected the fine stability of $Ru(bpy)_3^{2+}$/formaldehyde ECL system. After adding ozone, the ECL intensities decrease immediately and remain at low values during a period of 30 min. It indicates that the reaction process of formaldehyde and ozone is very fast.

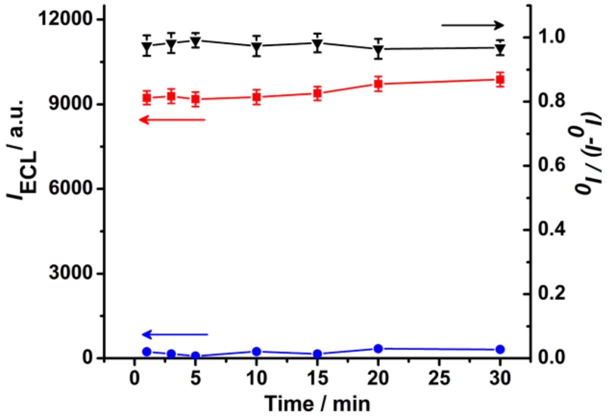

Fig. 4 Kinetic behavior of the ozone detection system at glassy carbon electrode. *I* (blue dots) represents the ECL intensity of the system after adding ozone; I_0 (red squares) represents the ECL intensity of the control sample; $(I_0 - I)/I_0$ (black triangles) represents the ECL inhibition efficiency after adding ozone. Conditions: *c*($Ru(bpy)_3^{2+}$): 1.0 mM; *c*(formaldehyde): 10 mM; *c*(ozone): 25 μM; PBS: 0.2 M, pH 10.0; Scan rate: 0.1 V/s, Photomultiplier tube voltage: 1000 V; time(min), 1, 3, 5, 10, 15, 20, 30.

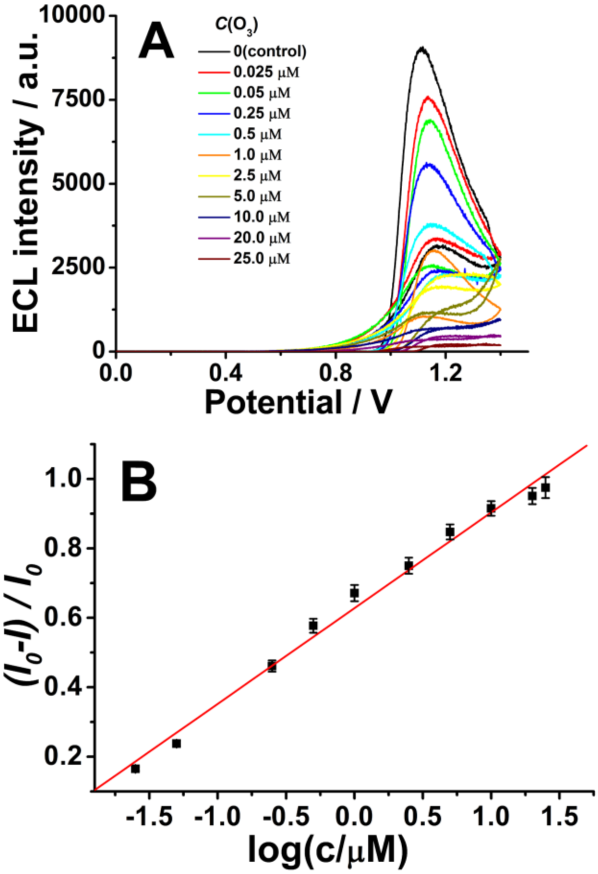

Fig. 5 ECL intensity-potential profiles (A) and linear relation (B) between ECL intensity and ozone concentration at glassy carbon electrode. Conditions: *c*($Ru(bpy)_3^{2+}$): 1.0 mM; *c*(formaldehyde): 10 mM; *c*(ozone): 0, 0.025, 0.05, 0.25, 0.5, 1, 2.5, 5, 10, 20, 25 μM; PBS: 0.2 M, pH 10.0; Scan rate: 0.1 V/s, Photomultiplier tube voltage: 1000 V.

Detection of ozone

Kinetic behaviors of the system were also investigated and shown in Fig. 3B. Fig. 5 shows the dependenc of ECL intensities on ozone concentrations. The ECL intensities increase as the concentrations of ozone increase as shown in Fig. 5.A. ECL inhibition efficiencies increase linearly with the concentrations of ozone (log *c*) from 0.025 μM to 25 μM with a correlation coefficient (r) of 0.9947. The regression equation is I = 0.6278 + 0.2757 log c(μM) and the limit of detection (LOD) is 8 nM. Moreover, the method has good reproducibility with a relative standard deviation (RSD, n = 7) of 2.9%. Table 1 compares our method with other methods. The proposed ECL method in this study is faster than most other methods and is more sensitive than other methods for the detection of ozone [7, 11, 12, 23, 32-34]. The present method shows better sensitivity than previous method using ECL of tris(1,10-phenanthroline)ruthenium(II)/glyoxal because of stronger ECL of $Ru(bpy)_3^{2+}$/formaldehyde [23].

Selectivity and recovery of the proposed method for the detection ozone

In addition to sensitivity, the selectivity of proposed method was investigated. Under the optimal conditions, a series of competing ROS or oxidants and some metal ions were investigated under similar conditions. As shown in Fig. 6, almost no enhancement of ECL intensity was observed, it is indicating that the ECL inhibition method for detection of ozone has very high selectivity.

The proposed method for the detection of ozone in a ventilated photocopy room was investigated. The recoveries for the addition of 1 and 10 μM ozone are 96.6% to 105.3% and 95.5% to 106.8%, respectively. The result showed that the proposed method is very promising for the detection of ozone.

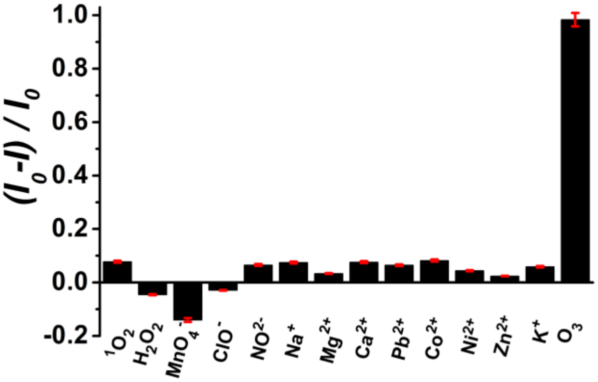

Fig. 6 ECL Selectivity of the proposed method for the detection of ozone. The other competing ROS or oxidants and some metal ions were investigated. I represents the ECL intensity of the system after adding ozone; I_0 represents the ECL intensity of the control sample; $(I_0 - I)/I_0$ represents the ECL inhibition efficiency after adding ozone. All of the concentrations of ozone and ROS or oxidants and metal ions are 20 μM. Conditions: $c(Ru(bpy)_3^{2+})$: 1.0 mM; c(formaldehyde): 10 mM; PBS: 0.2 M, pH 10.0; Scan rate: 0.1 V/s, Photomultiplier tube voltage: 1000 V.

Table 1. Comparison of different ozone detection methods.

Methods	Detection time	Linear ranges	LOD	Ref.
Indirect detection at the GC/MWCNT electrode based on the ozonolysis of indigo trisulfonate producing anthranilic acid	—	2.6–24 μM	0.2 μM	[34]
Fluorescence resonance energy transfer platform with a fluorescent RuSiNPs probe	10 min	0.7–35.0 μM	0.38 μM	[7]
Electrochemical detection using boron-doped diamond electrodes	—	0.49–740 μM	0.185 μM	[12]
ECL resonance energy transfer turn-on method	5 min	0.05–3.0 □ μM	30 nM	[35]
Fluorescence sensor based on ozone trapped by H_3BO_3-LK solution to produce iodine	—	0.08–53.3 □ μM	40 nM	[36]
Fluorescence sensor based on a twisted intramolecular charge transfer with a near-infrared Trp-Cy fluorescent probe	30 min	0.05–7.0 μM	17 nM	[11]
ECL sensor based on $Ru(phen)_3^{2+}$/glyoxal	1 min	0.05–25.0 μM	20 nM	[23]
ECL sensor based on $Ru(bpy)_3^{2+}$/formaldehyde system	1 min	0.025–25.0 μM	8 nM	Present work

Conclusion

This study shows that ozone can quench $Ru(bpy)_3^{2+}$ ECL using polymerizable coreactants including formaldehyde, methylglyoxal, and glyoxalate with remarkable efficiencies. The highly efficient quenching enables highly sensitive detection of ozone using the $Ru(bpy)_3^{2+}$/formaldehyde ECL system. Moreover, the method is rapid, simple and selective.

This study is helpful for developing other quenching systems and sensitive detection methods based on ECL quenching.

Acknowledgements

This project was supported by the National Natural Science Foundation of China (No. 21175126 and 21475123).

Notes and references

[a] School of Chemistry and Environmental Engineering, Changchun University of Science and Technology, Changchun 130022, China.
b State Key Laboratory of Electroanalytical Chemistry, Changchun Institute of Applied Chemistry, Chinese Academy of Sciences, Changchun, Jilin 130022, China.
c University of the Chinese Academy of Sciences, Chinese Academy of Sciences, No. 19A Yuquanlu, Beijing 100049, China.
*Corresponding author: Prof. Y.H. Li and G. Xu
†Tel/Fax: +86-431-85262747 (G. Xu); E-mail: liyh@cust.edu.cn (Y.H. Li), guobaoxu@ciac.ac.cn (G. Xu).

Electronic Supplementary Information (ESI) available: [details of any supplementary information available should be included here]. See DOI: 10.1039/b000000x/

1. D.-P. Yang, X. Wang, X. Guo, X. Zhi, K. Wang, C. Li, G. Huang, G. Shen, Y. Mei and D. Cui, *J. Phys. Chem. C*, 2014, **118(1)**, 725-731.
2. C. Lin, G. Wen, A. Liang and Z. Jiang, *RSC Adv.*, 2013, **3(18)**, 6627-6630.
3. K. Teranishi, Y. Shimada, N. Shimomura and H. Itoh, *Ozone Sci. Eng.*, 2013, **35(3)**, 229-239.
4. A. L. Garner, C. M. St Croix, B. R. Pitt, G. D. Leikauf, S. Ando and K. Koide, *Nat. Chem.*, 2009, **1(4)**, 316-321.
5. B. C. Dickinson and C. J. Chang, *Nat. Chem. Biol.*, 2011, **7(8)**, 504-511.
6. Q. Schiermeier, *Nature*, 2009, **460**, 792-795.
7. W. Qi, D. Wu, J. Zhao, Z. Liu, M. Xu, S. Anjum and G. Xu, *The Analyst*, 2013, **138(21)**, 6305-6308.
8. S. Huh, J. Park, Y. S. Kim, K. S. Kim, B. H. Hong and J.-M. Nam, *ACS Nano*, 2011, **5**, 9799-9806.
9. P. C. Andersen, C. J. Williford and J. W. Birks, *Anal. Chem.*, 2010, **82**, 7924-7928.
10. Y. Y. Maruo, T. Kunioka, K. Akaoka and J. Nakamura, *Sens. Actuators, B*, 2009, **135(2)**, 575-580.
11. K. Xu, S. Sun, J. Li, L. Li, M. Qiang and B. Tang, *Chem. Commun.*, 2012, **48(5)**, 684-686.
12. Y. Ishii, T. A. Ivandini, K. Murata and Y. Einaga, *Anal. Chem.*, 2013, **85(9)**, 4284-4288.
13. D. V. Stergiou, M. I. Prodromidis, P. G. Veltsistas and N. P. Evmiridis, *Anal. Chem.*, 2006, **78(13)**, 4676-4682.
14. L. Hu and G. Xu, *Chem. Soc. Rev.*, 2010, **39(8)**, 3275-3304.
15. W. Miao, *Chem. Rev.*, 2008, **108**, 2506-2553.
16. P. Bertoncello, A. J. Stewart and L. Dennany, *Anal. Bioanal. Chem.*, 2014, **406 (23)**, 5573-5587.
17. F. Li, Y. Yu, H. Cui, D. Yang and Z. Bian, *The Analyst*, 2013, **138**, 1844-1850.
18. X. Liu, L. Shi, W. Niu, H. Li and G. Xu, *Angew. Chem. Int. Ed.*, 2007, **46(3)**, 421-424.
19. Y. Koizumi and Y. Nosaka, *J. Phys. Chem. A*, 2013, **117**, 7705-7711.
20. P. Bertoncello and R. J. Forster, *Biosens. Bioelectron.*, 2009, **24 (11)**, 3191-3200.
21. W.-Y. Lee, *Mikrochim. Acta*, 1997, **127**, 19-39.
22. J. P. Choi and A. J. Bard, *Anal. Chim. Acta*, 2005, **541(1-2)**, 141-148.
23. L. Hu, H. Li, S. Zhu, L. Fan, L. Shi, X. Liu and G. Xu, *Chem. Commun.*, 2007**(40)**, 4146-4148.
24. W. Yao, L. Wang, H. Wang, X. Zhang and L. Li, *Biosens. Bioelectron.*, 2009, **24(11)**, 3269-3274.
25. W. Qi, Z. Liu, J. Lai, W. Gao, X. Liu, M. Xu and G. Xu, *Chem. Commun.*, 2014, **50(60)**, 8164-8166.
26. Y. Zhuo, N. Liao, Y. Q. Chai, G. F. Gui, M. Zhao, J. Han, Y. Xiang and R. Yuan, *Anal. Chem.*, 2014, **86(2)**, 1053-1060.
27. Y. Liao, R. Yuan, Y. Chai, Y. Zhuo, Y. Yuan, L. Bai, L. Mao and S. Yuan, *Biosens. Bioelectron.*, 2011, **26(12)**, 4815-4818.
28. R. Kurita, K. Arai, K. Nakamoto, D. Kato and O. Niwa, *Anal. Chem.*, 2012, **84(4)**, 1799-1803.
29. X.-M. Chen, B.-Y. Su, X.-H. Song, Q.-A. Chen, X. Chen and X.-R. Wang, *TrAC Trend Anal. Chem.*, 2011, **30(5)**, 665-676.
30. W. Qi, M. T. Gabr, Z. Liu, L. Hu, M. Han, S. Zhu and G. Xu, *Electrochim. Acta*, 2013, **89**, 139-143.
31. L. Hu, H. Li, S. Han and G. Xu, *J. Electroanal. Chem.*, 2011, **656(1-2)**, 289-292.
32. H. Cui, F. Li, M. Shi, Y. Pang and X. Lin, *Electroanalysis*, 2005, **17**, 589-598.
33. J. McCall, C. Alexander and M. M. Richter, *Anal. Chem.*, 1999, **71**, 2523-2527.
34. I. Cesarino, F. C. Moraes, S. A. S. Machado, J. PassarettiFilho and A. A. Cardosob, *Electroanalysis*, 2011, **23(6)**, 1512-1517.
35. W. Qi, D. Wu, J. Zhao, Z. Liu, W. Zhang, L. Zhang and G. Xu, *Anal. Chem.*, 2013, **85(6)**, 3207-3212.
36. Q. Liu, C. Lin, X. Zhang, G. Wen and A. Liang, *Luminescence*, 2014, **29(8)**, 1102-1106.